

Bimodal fluorescence signaling based on control of the excited-state conformational twisting and the ground-state protonation processes

Jye-Shane Yang,^{a,*} Chung-Yu Hwang^b and Mon-Yao Chen^b

^aDepartment of Chemistry, National Taiwan University, Taipei 10617, Taiwan

^bDepartment of Chemistry, National Central University, Chung-Li 32054, Taiwan

Received 25 December 2006; revised 16 February 2007; accepted 16 February 2007

Available online 1 March 2007

Abstract—Amino-based fluoroionophores **1** and **2** can selectively sense alkaline earth metal ions in MeCN under both neutral and acidic conditions by different signaling mechanisms. The fluoroionophoric behavior for the neutral probes is characterized by an ‘off-on’ photoinduced electron transfer (PET)-like fluorescence intensity response due to a switching from a twisted internal charge transfer (TICT) to a planar internal charge transfer (PICT) state. For the protonated probes (i.e., **1**/H⁺ and **2**/H⁺), the fluorescing species is the localized stilbene fluorophores, but dual fluorescence is induced upon metal-ion recognition through a deprotonation process.

© 2007 Elsevier Ltd. All rights reserved.

Development of fluorescent probes or chemosensors for biological and/or environmental applications continues to play a key role in the field of probe design, because fluorescence measurement is an inherently sensitive and practically simple technique.¹ Among the various fluorescence signaling mechanisms, the utilities of photo-induced electron transfer (PET)² and internal charge transfer (ICT)³ have been well demonstrated. For PET-based probes, dramatic changes in fluorescence intensity lead to either an ‘off-on’ (i.e., fluorescence enhancement) or an ‘on-off’ (i.e., fluorescence quenching) response.² In contrast, the sensing behavior of ICT-based probes is characterized by spectral shifts in both the absorption and fluorescence spectra, which allows ratiometric measurement.³ A particular type of ICT probes relies on the presence of a twisted ICT (TICT) state in addition to the normal planar ICT (PICT) state.^{4,5} When both the PICT and TICT states are fluorescent, the free probes show dual fluorescence. When the TICT state is predominant but nonfluorescent, the free probes would be weakly fluorescent, resembling the off state of PET-based probes. As a

result, the fluorescence signaling behavior for TICT-based probes might be an off-on or ratiometric type, depending on the nature of fluorophore.

The vast majority of the reported (T)ICT and PET probes adopt one or more amino group(s) as the electron donor (D).^{1–4} However, the operation of these amino-based probes generally requires careful pH control for success, and in most cases the signal function is invalidated under acidic conditions due to the protonation of the amino group. An additional problem associated with (T)ICT fluoroinophores of simple donor–acceptor (D–A) constitution is the phenomenon of excited-state ion decoordination, which reduces the probe sensitivity.⁶ We report herein new amino-based D–A typed fluoroionophores **1** and **2**, which can operate under both neutral and acidic conditions with high sensitivity to alkaline earth metal ions, particularly Mg²⁺, through different signaling mechanisms. Whereas the fluorescence response is mainly an off-on behavior under neutral conditions, dual fluorescence with ratiometric behavior is observed in the presence of 10 mM HClO₄.

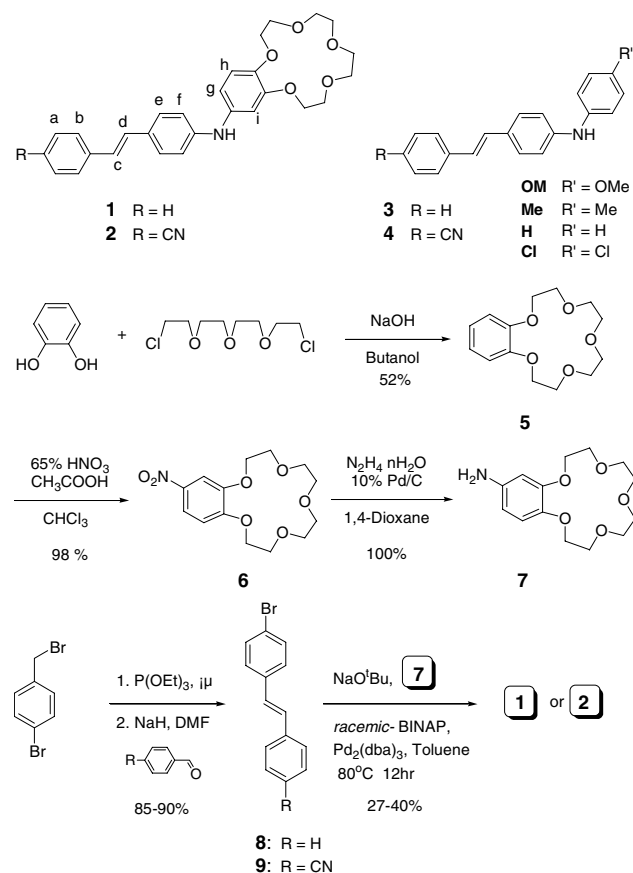
The design of fluoroionophores **1** and **2** was inspired by our recent works on the fluorescence behavior of *N*-aryl substituted aminostilbenes **3** and **4**.⁷ When the substituent in the *N*-aryl group of **3** or **4** (i.e., the R' group) is

Keywords: Fluoroionophores; Signaling; PET; TICT; PICT; Dual fluorescence.

*Corresponding author. Fax: +886 2 23636359; e-mail: jsyang@ntu.edu.tw

methoxy (i.e., **3OM** and **4OM**), the fluorescence quantum yield is rather low in acetonitrile ($\Phi_{\text{fl}} \sim 0.006$) due to the efficient formation of a weakly fluorescent TICT state. However, TICT-state formation is negligible for those with a less electron-donating or weak electron-withdrawing substituent such as methyl (**3Me** and **4Me**), hydrogen (**3H** and **4H**), or chloro (**3Cl**), leading to much higher fluorescence quantum yields ($\Phi_{\text{fl}} = 0.13\text{--}0.43$). Because of such a unique substituent effect, we consider that *trans*-4-(*N*-arylamino)stilbenes are potential TICT-based fluorescent probes upon introducing appropriate receptors at the *N*-aryl group. To test this hypothesis, benzocrown derivatives **1** and **2** were investigated. We reasoned that **1** and **2** might retain the weak fluorescence nature of **3OM** and **4OM**, and a small amount of electronic perturbation on the oxygen donor might be sufficient to 'turn on' the fluorescence of **1** and **2** through the inhibition of the TICT process. In addition, unlike the conventional PET and (T)ICT probes, the amino nitrogen in **1** and **2** is not a part of the receptor (i.e., ionophore), which might minimize the potential influence of excited-state cation decoordination.

The synthesis of **1** and **2** is shown in Scheme 1. Intermediates **5–9** are all known compounds.⁸ Their preparations were carried out by following the literature procedures and their characterization data conform to the reported values. Palladium-catalyzed amination reactions⁹ between **8** or **9** and **7** provided the desired compounds **1** and **2**.¹⁰



Scheme 1.

Table 1 shows the maxima of absorption and fluorescence spectra and fluorescence quantum yield (Φ_{fl}) for **1** and **2** along with the data of **3** and **4** in acetonitrile. The photophysical data for **1** and **2** are all similar to those for **3OM** and **4OM**, respectively, except for the fluorescence maxima for **2** versus **4OM**. This indicates that the presence of an additional alkoxy group at the *meta*-position of the *N*-(4-anisole) group does not affect the TICT process. Since the fluorescence spectra for **1**, **2**, **3OM**, and **4OM** result from an unresolved overlapping of the PICT and the TICT fluorescence,⁷ the fluorescence maxima would depend on the relative intensity of the PICT and TICT fluorescence. Thus, the difference in the fluorescence maxima between **2** (547 nm) and **4OM** (583 nm) can be attributed to a relatively stronger fluorescence for the PICT than the TICT for **2** versus **4OM**, because the PICT fluorescence is blue shifted relative to the TICT fluorescence.

Figure 1 shows the absorption and fluorescence titration spectra of **1** and **2** in MeCN with Mg^{2+} . Whereas the absorption spectra are little affected, the fluorescence spectra are blue shifted by 25–52 nm and the fluorescence intensity is increased by as large as 54–70 times (i.e., switching 'on' the fluorescence) when the concentration of Mg^{2+} is 150 μM . Apparently, complexation between the benzocrown and Mg^{2+} (vide infra) perturbs the electron-donating ability of the crown oxygens and in turn the overall electron-donating ability of the aryl-amino group. Such a perturbation on the electron donor is sufficient to inhibit the TICT process, and thus the fluorescing state becomes the highly fluorescent PICT state due to the amino-conjugation effect.¹¹ It should be noted that the significant fluoroionophoric behavior for **1** and

Table 1. Absorption maxima (λ_{abs}), fluorescence maxima (λ_{fl}), fluorescence quantum yield (Φ_{fl}), and binding constants ($\log K$) for compounds **1–4** and for the complexes of **1** and **2** in MeCN

Compound ^a	λ_{abs} (nm)	λ_{fl} (nm)	Φ_{fl}^b	$\log K$
1	355	497	0.007	
1 / Mg^{2+}	350	445	0.38 (54)	4.2
1 / Ca^{2+}	351	447	0.29 (41)	4.1
1 / Sr^{2+}	351	455	0.22 (31)	3.9
1 / Ba^{2+}	351	456	0.13 (19)	3.8
1 / H^+	298, 310	358		3.1
2	386	547	0.002	
2 / Mg^{2+}	378	522	0.14 (70)	5.2
2 / Ca^{2+}	377	525	0.07 (35)	5.0
2 / Sr^{2+}	377	531	0.04 (20)	4.8
2 / Ba^{2+}	379	536	0.02 (10)	4.7
2 / H^+	318, 383	363, 522		3.0
3OM ^c	356	502	0.007	
3Me ^c	354	457	0.41	
3H ^c	351	442	0.34	
3Cl ^c	351	437	0.43	
4OM ^d	384	583	<0.005	
4Me ^d	382	531	0.13	
4H ^d	379	504	0.35	

^a The counter anion for the cation is perchlorate (ClO_4^-).

^b Value in the parentheses is the fluorescence enhancement factor relative to the free probe (i.e., Φ_{fl}/Φ_0 , where Φ_0 is the Φ_{fl} for the free probe).

^c Data from Ref. 7a.

^d Data from Ref. 7b.

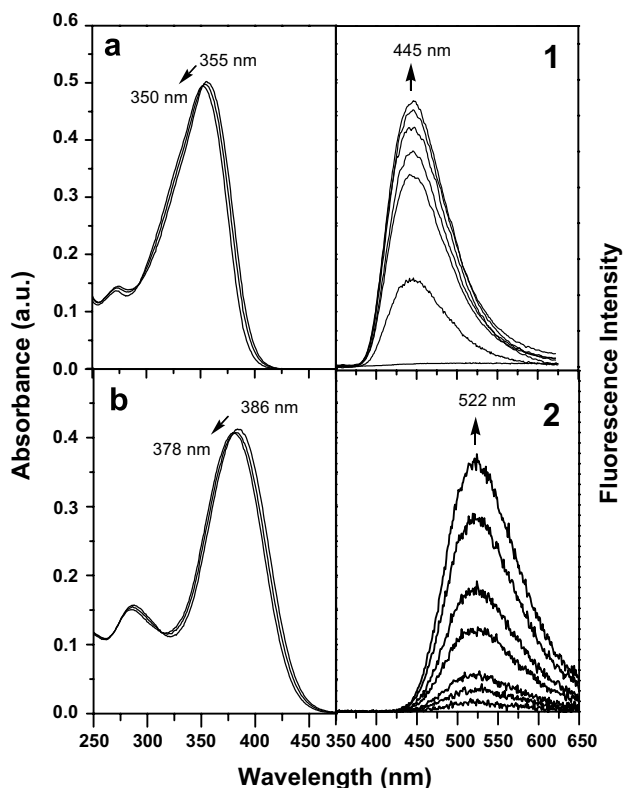


Figure 1. Absorption and fluorescence spectra of (a) **1** (1×10^{-5} M excitation at 325 nm) and (b) **2** (1×10^{-5} M, excitation at 340 nm) in MeCN upon addition of 0, 1, 3, 5, 10, 15, 30 equiv of $\text{Mg}(\text{ClO}_4)_2$. For clarity, the absorption spectra are shown at 0, 5, and 30 equiv of $\text{Mg}(\text{ClO}_4)_2$.

2 does not necessarily indicate the absence of any excited-state cation decoordination behavior. It is more likely that the cation decoordination effect is smaller for **1** and **2** than those where the amino nitrogen participates in the cation binding. Provided that the electron-donating ability for the donors in the complex forms of **1** and **2** is far off the threshold for TICT formation, a small degree of cation decoordination would not resume the TICT process. As shown by the case of **2**, recognition of Mg^{2+} by the benzocrown moiety is supported by the ^1H NMR spectra (spectra a and b in Fig. 2), where the benzocrown protons display a much larger downfield shifting ($\Delta\delta = 0.2\text{--}0.4$ ppm) than the rest of the protons ($\Delta\delta < 0.1$ ppm).

Compounds **1** and **2** also display fluorescence responses to the other alkaline earth metal ions Ca^{2+} , Sr^{2+} , and Ba^{2+} , but the size of the spectral shifts and intensity enhancement is relatively lower than the case of Mg^{2+} . In contrast, little or no fluorescence responses were found for alkali metal ions such as Li^+ , Na^+ , and K^+ . The larger fluorescence response of **1** and **2** to Mg^{2+} versus the other metal ions could be attributed to its higher charge density (e.g., Mg^{2+} (0.75) $>$ Ca^{2+} (0.24)).¹² As exemplified by the case of **1**, the ion selectivity based on the intensity-ratio plot of the fluorescence quantum yields against the concentration of these metal ions is depicted in Figure 3a. According to the Job plots based on the changes in fluorescence (Fig. 3b), a 1:1 complex is

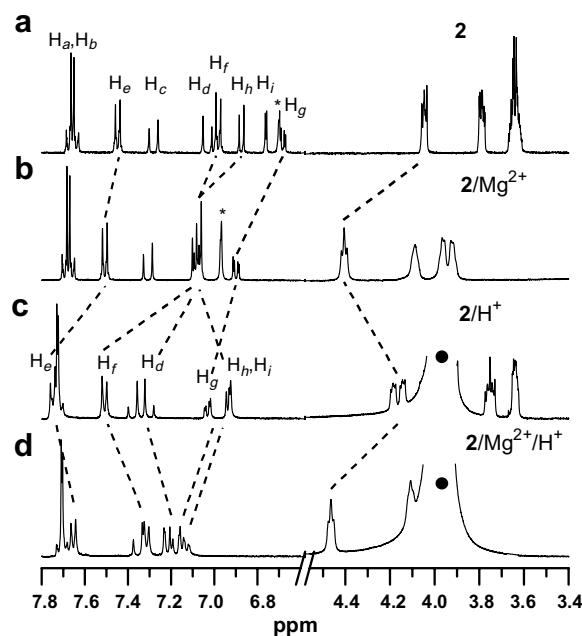


Figure 2. ^1H NMR spectra (400 MHz) of (a) **2**; (b) $2/\text{Mg}^{2+}$; (c) $2/\text{H}^+$; and (d) $2/\text{Mg}^{2+}/\text{H}^+$ in acetonitrile- d_3 (counter ion ClO_4^-). The concentration for **2**, Mg^{2+} , and H^+ are 1, 10, and 10 mM, respectively. The marks * and ● denote the peaks of NH and the excess H^+ , respectively, and the dash lines are to correlate the shifting of specific proton signals. See the molecular structure for the designation of protons.

formed between the fluoroionophores and the alkaline earth metal ions at low concentrations (the total concentration is at 1×10^{-5} M). Their binding constants, expressed as $\log K$, determined by absorption titration spectra¹³ along with the spectral data for **1** and **2** are reported in Table 1.

Interestingly, the function of **1** and **2** is not interfered even under highly acidic conditions, but the signaling mechanism is distinct (Fig. 4). As exemplified by the case of **1**, the fluorescence spectra undergo a large blue shift ($\Delta\lambda_{fl} = 139$ nm) in the presence of 10 mM HClO_4 , and the fluorescence spectrum resembles that for a simple stilbene fluorophore. Thus, a full protonation of the amino group in the ground as well as the excited state is indicated. Upon addition of Mg^{2+} , the PICT fluorescence band is generated, leading to dual fluorescence. Apparently, the coordination of Mg^{2+} expels the ammonium proton, presumably due to charge–charge repulsions. The phenomenon of metal-ion induced deprotonation of the ammonium ion that triggers a PET process and thus quenches the fluorescence has recently been reported.¹⁴ However, the deprotonation behavior that triggers an ICT process and leads to dual fluorescence is unprecedented. The corresponding ratio-metric plot against the concentration of metal ions for **1** is shown in Figure 5. It should also be noted that at lower concentration of HClO_4 such as 1 mM the fluorescence signaling behavior resembles that under neutral conditions. In other words, fluoroionophore **1** has little responses to or affected by protons at low concentrations, as demonstrated by the case of **1** to Mg^{2+} (Fig. 3a). This phenomenon can be attributed to the

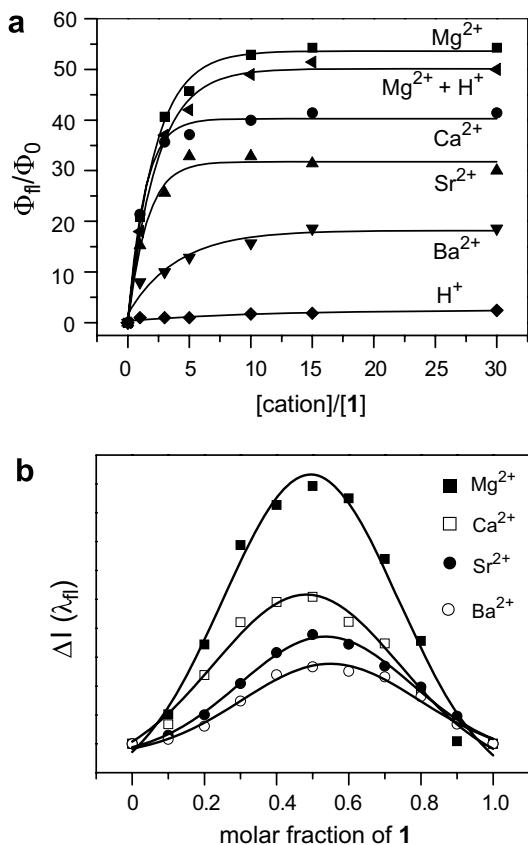


Figure 3. (a) The plot of changes in the ratio of the fluorescence quantum efficiency (Φ_f/Φ_0 , where Φ_0 is the Φ_f for the free probe) against the ratio of the concentration of alkaline earth metal ions Mg^{2+} , Ca^{2+} , Sr^{2+} , Ba^{2+} , and proton (counter ion ClO_4^-) versus **1** (1×10^{-5} M, excitation at 325 nm) in MeCN, and (b) the Job plot of **1** with metal ions in MeCN (the total concentration of **1** and metal ions is 1×10^{-5} M).

weak basicity of diarylamines and thus the low proton binding constants (Table 1). Similar fluoroionophoric behavior was also observed for **2** (Fig. 4b). The above-proposed fluorescence sensing mechanisms are supported by the ^1H NMR studies based on **2**. As shown in Figure 2, H^+ induces a much larger downfield shifting for the protons in the diphenylamino group than the other protons (spectrum c in Fig. 2), which is explicitly different from the effect of Mg^{2+} and consistent with the protonation of the amino nitrogen. When Mg^{2+} was added at such an acidic condition, the signals of protons H_d – H_f shifts upfield to a significant extent ($\Delta\delta = 0.1$ – 0.2 ppm), but the benzocrown protons undergo downfield shifting with a size similar to that in neutral conditions (spectrum d in Fig. 2), a behavior consistent with the phenomenon of Mg^{2+} -binding-induced deprotonation reaction.

The difference in fluorescence properties between **1** and **2** deserves our attention. When compared to **1**, the presence of an electron-withdrawing cyano group in the stilbene moiety for **2** enhances the ICT character and thus results in a red shift in the spectra and reduces the fluorescence quantum efficiency. Regarding the fluoroionophoric behavior, the selectivity and sensitivity toward

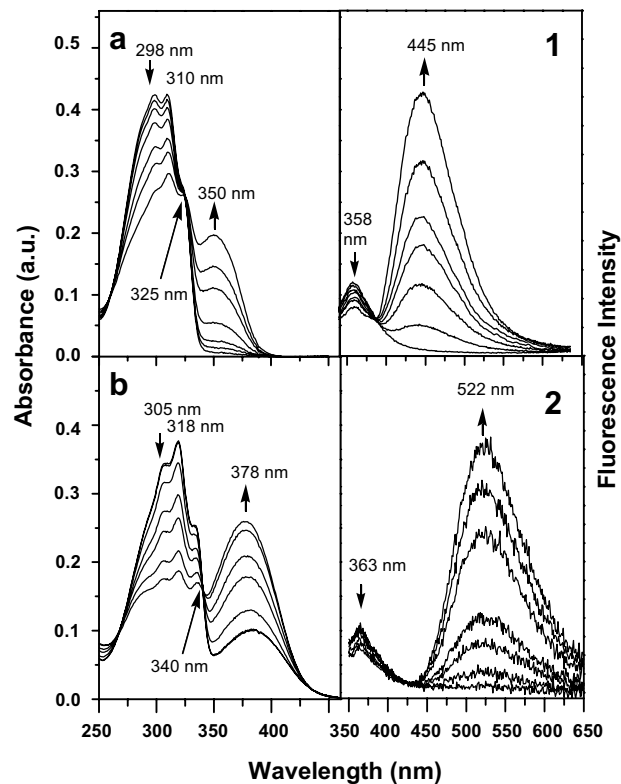


Figure 4. Absorption and fluorescence spectra of (a) **1** (1×10^{-5} M, excitation at the isosbestic point, 325 nm) and (b) **2** (1×10^{-5} M, excitation at the isosbestic point, 340 nm) in MeCN with 0.01 M of HClO_4 upon addition of 0, 1, 3, 5, 10, 15, 30 equiv of $\text{Mg}(\text{ClO}_4)_2$.

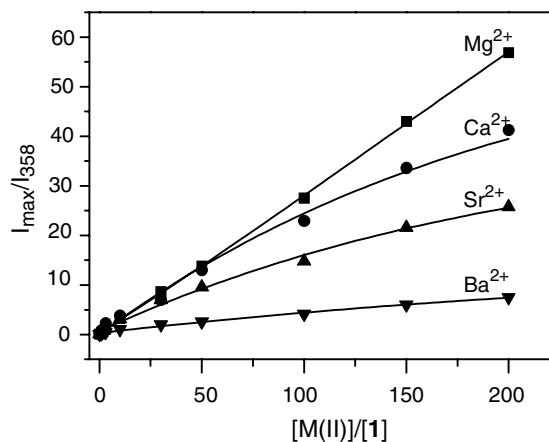


Figure 5. The plot of changes in the ratio of the intensity of fluorescence maxima (I_{max}/I_{358} , where I_{max} is the fluorescence maxima in the presence of metal ions) against the ratio of the concentration of alkaline earth metal ions Mg^{2+} , Ca^{2+} , Sr^{2+} , and Ba^{2+} and proton versus **1** (1×10^{-5} M, excitation at 325 nm) in MeCN with 0.01 M of HClO_4 .

Mg^{2+} appears to be slightly better for **2** versus **1** (Table 1) under neutral conditions. The higher sensitivity is illustrated by the higher fluorescence enhancement factor (70 vs 54), and the higher selectivity is evidenced by the larger reduction in the fluorescence enhancement

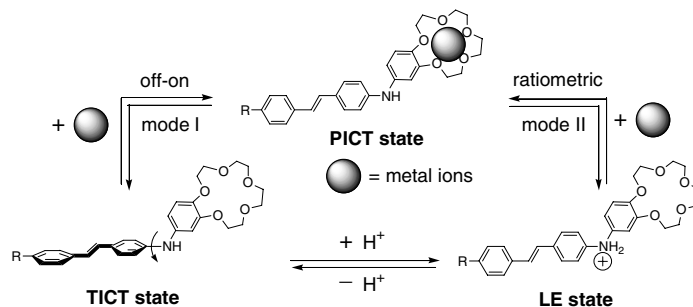


Figure 6. Schematic presentation of the bimodal fluoroinophoric behavior of **1** and **2**.

factor on going from Mg^{2+} to Ca^{2+} and to Ba^{2+} . Under the acidic conditions, the absorption band for the free probe (386 nm) is not completely disappeared (Fig. 3), which can be accounted for by the lower basicity of **2** due to the cyano group.

In conclusion, we have demonstrated that *trans*-4-(*N*-arylamino)stilbenes are potential fluorophores for sensor design. In particular, as shown by the benzocrown derivatives **1** and **2**, the resulting fluorescent probes can function under acidic as well as neutral conditions through different signaling mechanisms. The summarized fluoroionophoric behavior for **1** and **2** is depicted in Figure 6. Whereas the fluorescence response of **1** and **2** is a combination of an off–on intensity changes and wavelength shifts under neutral conditions, fluorescence signaling under acidic conditions results in metal ion-induced deprotonation of the ammonium ion and LE-PICT dual fluorescence. Since the selectivity of a probe and the complex stability mainly depend on the receptor, the use of more selective and powerful receptors should improve the performance (e.g., function in aqueous solutions) of *N*-(arylamino)stilbene-derived fluorescent probes. Further investigation toward this issue is in progress.

Acknowledgment

Financial support for this research was provided by the National Science Council of Taiwan, ROC.

References and notes

- (a) de Silva, A. P.; Gunaratne, H. Q. N.; Gunnlaugsson, T.; Huxley, A. J. M.; McCoy, C. P.; Rademacher, J. T.; Rice, T. E. *Chem. Rev.* **1997**, *97*, 1515–1566; (b) Valeur, B.; Leray, I. *Coord. Chem. Rev.* **2000**, *205*, 3–40; (c) de Silva, A. P.; Fox, D. B.; Huxley, A. J. M.; Moody, T. S. *Coord. Chem. Rev.* **2000**, *205*, 41–57; (d) GoKel, G. W.; Leevy, W. M.; Weber, M. E. *Chem. Rev.* **2004**, *104*, 2723–2750.
- For recent examples of PET-based probes, see: (a) Yang, J.-S.; Lin, Y.-D.; Lin, Y.-H.; Liao, F.-L. *J. Org. Chem.* **2004**, *69*, 3517–3525; (b) Chen, G.; Yee, D. J.; Gubernator, N. G.; Sames, D. *J. Am. Chem. Soc.* **2005**, *127*, 4544–4545; (c) Ghosh, K.; Masanta, G. *Tetrahedron Lett.* **2006**, *47*, 2365–2369; (d) Kim, H. J.; Kim, J. S. *Tetrahedron Lett.* **2006**, *47*, 7051–7055; (e) Ueno, T.; Urano, Y.; Kojima, H.; Nagano, T. *J. Am. Chem. Soc.* **2006**, *128*, 10640–10641.
- For recent examples of ICT-based probes, see: (a) Yang, J.-S.; Hwang, C.-Y.; Hsieh, C.-C.; Chiou, S.-Y. *J. Org. Chem.* **2004**, *69*, 719–726; (b) Yang, J.-S.; Lin, Y.-D.; Chang, Y.-H.; Wang, S.-S. *J. Org. Chem.* **2005**, *70*, 6066–6073; (c) Caballero, A.; Martínez, R.; Lloveras, V.; Ratera, I.; Vidal-Gancedo, J.; Wurst, K.; Tárraga, A.; Molina, P.; Veciana, J. *J. Am. Chem. Soc.* **2005**, *127*, 15666–15667; (d) Cheung, S.-M.; Chan, W.-H. *Tetrahedron* **2006**, *62*, 8379–8383; (e) Liu, L.-H.; Zhang, H.; Li, A.-F.; Xie, J.-W.; Jiang, Y.-B. *Tetrahedron* **2006**, *62*, 10441–10449.
- (a) Létard, J.-F.; Delmond, S.; Lapouyade, R.; Braun, D.; Rettig, W.; Kreissler, M. *Recl. Trav. Chim. Pays-Bas* **1995**, *114*, 517–527; (b) Collins, G. E.; Choi, L.-S.; Callahan, J. H. *J. Am. Chem. Soc.* **1998**, *120*, 1474–1478; (c) Choi, L.-S.; Collins, G. E. *Chem. Commun.* **1998**, 893–894; (d) Morozumi, T.; Anada, T.; Nakamura, H. *J. Phys. Chem. B* **2001**, *105*, 2923–2931; (e) Sibert, J. W.; Forshee, P. B. *Inorg. Chem.* **2002**, *41*, 5928–5930; (f) Aoki, S.; Kagata, D.; Shiro, M.; Takeda, K.; Kimura, E. *J. Am. Chem. Soc.* **2004**, *126*, 13377–13390; (g) Liu, B.; Chen, J.; Yang, G.; Li, Y. *Res. Chem. Intermed.* **2004**, *30*, 345–353; (h) Li, Y. Q.; Bricks, J. L.; Resch-Genger, U.; Spieles, M.; Rettig, W. *J. Fluoresc.* **2006**, *16*, 337–348.
- The PICT state often refers to the locally excited (LE) state.
- (a) Crochet, P.; Malval, J.-P.; Lapouyade, R. *Chem. Commun.* **2000**, 289–290; (b) Rurack, K.; Rettig, W.; Resch-Genger, U. *Chem. Commun.* **2000**, 407–408; (c) Malval, J.-P.; Gosse, I.; Morand, J.-P.; Lapouyade, R. *J. Am. Chem. Soc.* **2002**, *124*, 904–905.
- (a) Yang, J.-S.; Liao, K.-L.; Wang, C.-M.; Hwang, C.-Y. *J. Am. Chem. Soc.* **2004**, *126*, 12325–12335; (b) Yang, J.-S.; Liao, K.-L.; Hwang, C.-Y.; Wang, C.-M. *J. Phys. Chem. A* **2006**, *110*, 8003–8010.
- (a) Bance, S.; Barber, H. J.; Woolman, A. M. *J. Chem. Soc.* **1943**, 1–4; (b) Kumari, N.; Kendurkar, P. S.; Tewari, R. S. *J. Organomet. Chem.* **1975**, *96*, 237–241; (c) Berezina, R. N.; Kobrin, V. S.; Kusov, S. Z.; Lubenets, E. G. *Russ. J. Org. Chem.* **1998**, *34*, 1517–1518; (d) Bogaschenko, T.; Basok, S.; Kulygina, C.; Lyapunov, A.; Lukyanenko, N. *Synthesis* **2002**, 2266–2270.
- (a) Wolfe, J. P.; Wagaw, S.; Marcoux, J.-F.; Buchwald, S. L. *Acc. Chem. Res.* **1998**, *31*, 805–818; (b) Hartwig, J. F. *Angew. Chem., Int. Ed.* **1998**, *37*, 2046–2067.
- Typical synthetic procedures for aminostilbenes have been reported.¹¹ Characterization data for compounds **1** and **2** are shown in the following: Compound **1**: yield 27%; mp 68–69 °C; ¹H NMR (400 MHz CDCl₃) 3.80–3.82 (m, 8H), 3.93–3.95 (m, 4H), 4.11–4.17 (m, 4H), 6.69 (dd, *J* = 2.2 and 8.4 Hz, 1H), 6.74 (d, *J* = 2.2 Hz, 1H), 6.86 (d, *J* = 8.4 Hz, 1H), 6.95 (d, *J* = 8.4 Hz, 2H), 6.98 (d, *J* = 16.3 Hz, 1H), 7.08 (d, *J* = 16.3 Hz, 1H), 7.25 (t, *J* = 7.2 Hz, 1H), 7.37 (t, *J* = 7.5 Hz, 2H), 7.42 (d, *J* = 8.4 Hz, 2H), 7.51 (d,

$J = 7.8$ Hz, 2H) ppm; ^{13}C NMR (100 MHz CDCl_3): 68.85, 69.55, 69.80, 69.97, 70.49, 70.67, 70.99, 71.03, 107.32, 112.92, 115.83, 116.07, 125.66, 126.17, 127.03, 127.70, 128.45, 128.64, 129.14, 136.52, 137.86, 144.32, 144.72, 150.07 ppm; IR (KBr) 3244, 1599, 1513, 939 cm^{-1} ; FAB-HRMS calcd for $\text{C}_{28}\text{H}_{31}\text{NO}_5$: 461.2202. Found: 461.2198. Compound **2**: yield 40%; mp 74–75 °C; ^1H NMR (400 MHz, CD_2Cl_2) 3.66–3.70 (m, 8H), 3.83–3.84 (m, 4H), 4.04–4.07 (m, 4H), 5.83 (bs, 1H), 6.69 (d, $J = 8.5$ Hz, 1H), 6.72 (d, $J = 2.3$ Hz, 1H), 6.84 (d, $J = 8.5$ Hz, 1H), 6.93 (d, $J = 8.6$ Hz, 2H), 6.94 (d, $J = 16.3$ Hz, 1H), 7.16 (d, $J = 16.3$ Hz, 1H), 7.40 (d, $J = 8.6$ Hz, 2H), 7.55 (d, $J = 8.4$ Hz, 2H), 7.60 (d, $J = 8.4$ Hz, 2H) ppm; ^{13}C NMR (100 MHz, CD_2Cl_2): 69.02, 69.60, 69.84, 69.93, 70.48,

70.63, 71.02, 71.06, 108.01, 109.97, 113.55, 115.63, 115.70, 119.43, 123.45, 126.65, 127.97, 128.54, 132.42, 132.72, 136.04, 142.82, 145.41, 145.89, 150.32 ppm; IR (KBr) 3230, 2217, 1590, 1511, 938 cm^{-1} ; FAB-HRMS calcd for $\text{C}_{29}\text{H}_{30}\text{N}_2\text{O}_5$: 486.2155. Found: 486.2156.

11. Yang, J.-S.; Chiou, S.-Y.; Liao, K.-L. *J. Am. Chem. Soc.* **2002**, *124*, 2518–2527.
12. Watanabe, S.; Ikishima, S.; Matsuo, T.; Yoshida, K. *J. Am. Chem. Soc.* **2001**, *123*, 8402–8403.
13. Connors, K. A. *Binding Constants—The measurement of Molecular Complex Stability*; John Wiley & Sons: New York, 1987; Chapter 4.
14. Bu, J.-H.; Zheng, Q. U.; Chen, C.-F.; Huang, Z. T. *Org. Lett.* **2004**, *6*, 3301–3303.